Investigation on the behaviour of a thermo-active diaphragm wall by thermo-mechanical analyses

Donatella Sterpi [a,b,*], Andrea Coletto [a], Luca Mauri [a]

[a] *Department of Civil and Environmental Engineering, Politecnico di Milano, Italy*

[b] *P. Leonardo da Vinci, 32, 20133 Milano, Italy*

The thermo-active diaphragm walls are traditional retaining structures that embed heat exchangers for the exploitation of the near surface geothermal energy, used in the thermal conditioning of buildings and infrastructures. The coupled energetic and structural function of these so called energy walls requires some investigation in order to optimize the embedded circuit and assess the possible occurrence of significant consequences, in terms of temperature variations within the soils mass and thermal effects on the stress/strain state of the structure. In this contribution, the behaviour of an energy wall is assessed by finite element thermal analyses, that allow to investigate the energy performance and the short and long term influence on the soil temperatures, and by finite element thermo-mechanical analyses, to highlight the wall geotechnical and structural response. A one year cycle of heating/cooling operating mode of the geothermal system has been considered and the effects have been discussed in terms of soil–structure interaction and structural internal actions. The results show that the thermally induced mechanical effects are not negligible, especially as variations of the internal axial forces and bending moments. Although they seem to be not detrimental to the geotechnical and structural safety, they require a careful evaluation in order to predict possible situations of unexpected overstress conditions.

Keywords: Heat transfer, Ground temperature, Geothermal energy, Energy geostructure, Thermo-mechanical analysis, Finite element analysis

HIGHLIGHTS

- The layout of the exchanger pipe loop governs the energy performance.
- A realistic definition of the thermal boundary conditions and thermal inputs at the pipe inlet is crucial.
- The thermally induced variations of the wall axial forces and bending moments are not negligible.
- Different cross sections of the wall behave differently and mutually interact.
- A three-dimensional analysis is required, instead of the more conventional plane strain analysis.

1. Introduction

Recent statistics report that the worldwide energy supply and consumption have more than doubled over the last forty years and that fossil fuels still cover more than 80% of the total energy supply.[1] The energy demand is expected to increase due to the demographic and economic growth of large geographic areas of the developing world.

* Corresponding author.
E-mail addresses: donatella.sterpi@polimi.it (D. Sterpi), andrea.coletto@mail.polimi.it (A. Coletto), luca1.mauri@mail.polimi.it (L. Mauri).

Published Journal Article available at http://dx.doi.org/10.1016/j.gete.2016.10.001

The production and consumption of energy based on fossil fuels are responsible for large part of greenhouse gases and air pollutants, with consequent environmental and climate impacts. The use of renewable and green energy sources nowadays represents a necessary choice in order to cope with the growing energy demand, with the predictably increasing energy costs, and with the need for an environmentally sustainable progress. Among these sources, the geothermal energy represents an efficient solution for its massive potential, the steadiness with respect to the variable atmospheric conditions, the low environmental impact and the cost competitiveness. If in actual fact deep geothermal reservoirs, exploited for electrical energy production, can be localized only in particular geographic areas, the geothermal energy at low depths or at the near-surface, for direct use as thermal energy, is pervasively available.[2] This characteristic makes it optimal for a local harvesting and diffuse distribution.

Building and space heating and cooling technology is among the most important direct applications of shallow geothermal energy. In fact, the sector of buildings and spaces for domestic, commercial and public service use, has surpassed the sectors of industry and transport, heating currently accounts for 40% of building energy demand, and the cooling demand is expected to rise significantly in the next years.[1,3] In addition, buildings have an impact on long-term energy consumption, due to their long renovation cycle, for which reason new buildings should be designed in respect of a high energy performance. The majority of energy consumption takes place in the centre of large urban areas, due to their higher population density and higher living standards. District heating and cooling systems may therefore represent a critical infrastructure where renewable energy sources could be used in an integrated system.[4] In this framework, the use of near-surface geothermal energy is crucial for meeting the European targets about renewable energy exploitation and greenhouse gas emissions reduction.[5]

The so called energy geostructures are conventional reinforced concrete elements, embedded in the ground and designed to serve a primary structural function, that are in addition thermally active since they host heat exchanger pipes with the purpose to use the subsoil to disperse heat in summer and extract heat in winter. This system, although basically limited to the new constructions, offers the advantage of using existing structural components without requiring additional works and the availability of additional areas, with the associated costs. The energy geostructures can provide thermal conditioning to buildings and spaces and also to large infrastructures, such as airport runways and bridge decks, to mitigate the effects of high temperatures in summer or freezing temperatures in winter.[6,7]

In general, the challenges in the design of energy geostructures stem from their coupled structural and energetic function and from the strict connection of several disciplines,[8,9] as outlined by the broad spectrum contributions in Laloui and Di Donna,[10] and in the comprehensive review by Brandl.[11] Thermo-active piles were the first geostructures to be designed in the 80s mainly in Austria, closely followed by diaphragm walls and floor slabs, often associated with the cut-and-cover construction of shallow tunnels.[12–16] In the 2000, the technology spreads to bored tunnels segmental liners[17–20] and, more recently, to anchors for tunnel reinforcement and retaining walls.[21]

The energy performance of these geostructures firstly depends on the ground hydro-geological conditions and thermal properties. The preliminary investigation can be considered similar to the one conventionally carried out for the design of shallow ground source thermal systems, aimed at recognizing the subsoil and the excavation feasibility, especially in urban areas.[22–24] The thermal properties can be identified from the properties of the soil constituent phases or from on site thermal response tests.[25,26] The energy performance depends also on the geometry of the geostructure, i.e. the overall surface extension on which the heat transfer can take place, the depth that the geostructure reaches, and the presence of exposed surfaces. For instance, piles can reach high depths, diaphragm walls have a wide surface extension and tunnels take advantage of both depth and surface extension. In addition, piles are fully embedded, while diaphragm walls and tunnels have exposed surfaces with specific conditions of heat flux.[27] Finally, an analysis is required about the climate conditions and the building physics, including the natural thermal energy transfer between the building and the atmosphere and the building and the ground.[28,29]

The role of the groundwater flow has been considered firstly for traditional borehole heat exchangers[30] and then for geostructures such as piles, diaphragm walls and tunnels.[7,31–33] A positive influence of the flow in high permeability soils has been recognized whenever there is a need to seasonally restore the ground thermal energy, i.e. when the geothermal system is used yearly in one season only, for either cooling or more often heating. Conversely, when it is used in dual operating mode and the soil works as seasonal thermal energy storage mass, the groundwater flow is detrimental to the system efficiency.

The behaviour of thermo-active piles, or energy piles, has been largely investigated, in terms of both energy efficiency and thermo-mechanical response. Monitoring data from instrumented full scale energy piles[13,34,35] provided major insights in the geotechnical and structural consequences of the heat transfer and established important databases for the validation of numerical analyses and the calibration of the relevant parameters.[36–39] Taking advantage of ideal, controlled and repeatable conditions, also laboratory tests on small scale models helped in identifying the pile response capacity.[40–44] The thermal effects represent additional contributions to the mechanical loads and highly depend on the level of constraint that the soil exerts on the pile in terms of lateral friction and base bearing.

Similar consequences are also expected in thermo-active reinforced concrete diaphragm walls, briefly referred to as energy walls, but the effects of thermal loads on energy walls are less investigated and also less predictable than on energy piles, due to a greater complexity in geometry and constraints and uncertainties in the thermal boundary conditions. For the same reasons, also heat transfer models developed for borehole heat exchangers or energy piles cannot be straightforwardly extended to energy walls and suitable models need to be introduced. In order

to solve the problems related to the complex configuration of energy walls, Kürten et al.[32] discuss a novel thermal resistance model and validate it against both numerical analyses with fully meshed domain and laboratory tests on reduced scale models, while Sun et al.[45] introduce a new design method and compare the analytical predictions with numerical solutions and field monitoring data. The latter were obtained from an experimental campaign aimed at investigating various key impact factors on the energy performance of diaphragm walls in Shanghai Museum of Natural History.[16]

Few case histories of energy walls, with reference to both bored pile walls and panel walls, are reported in the literature with a focus on both energy and structural performance. In the reported case of Lainzer tunnel (Vienna, Austria), a bored pile wall was instrumented to record variations in temperature field and strain state, but not in the stress state.[11] The recorded data show that the temperature induced strains are smaller than those induced by the excavation, and that the temperature variations due to the heat transfer are smaller than those due to natural fluctuations.

In Vienna U2/2-Taborstraβe Metro station a geothermal cooling system involving diaphragm walls and base slabs was implemented to dissipate into the ground a significant waste heat.[11,46] A preliminary feasibility study demonstrated that the temperature variations have a negligible effect on the load-bearing capacity of the soil and the building components. A set of strain gauges and chain extensometers, together with temperature sensors, was installed within the panels to check the wall structural behaviour.

The effect of heating and cooling on the short and long term structural performance of an energy wall was investigated also by Soga et al.[47] for the case of Tottenham Court Road station in the Crossrail in London. From the predictions of 2D thermo-hydro-mechanical finite element analyses the most relevant effects seem to be the concrete strains induced by a thermal differential in the wall thickness, the variations in earth pressures on the wall, and the soil shrinkage or expansion due to a ground thermal drift in the long term.

Two-dimensional thermo-mechanical finite element analyses are also carried out by Habert and Burlon,[48] who reach a preliminary conclusion about the limited effect of the temperature variations on the behaviour of the wall, which still meets the requirements for geotechnical safety. Numerical analyses carried out by Bourne-Webb et al.[49] report that, for all the cases considered, the effects of heating and cooling operations on the mechanical response are minor compared with the changes attributable to the natural climatic fluctuations.

In all the reported cases, the thermal boundary conditions and the heating/cooling inputs, related to the building energy demand, proved to be crucial parameters influencing the performance of the energy wall.

This paper aims at contributing to the understanding of the energy performance and of the thermal effects on the structural behaviour of energy walls. The differences between energy piles and energy walls will be outlined in order to highlight the particular features of energy walls. Then, the results of a preliminary study will be discussed, from the perspective of both the geothermal energy exploitation and the short and long term influence on the ground temperatures. Finally, the effects of the heat transfer process on the energy wall and on the soil–structure interaction are investigated by 3D thermo-mechanical finite element analyses. The discussion of the numerical results allows to get insights into the thermally induced stresses that, ultimately, affect the wall deformation, the earth pressure distribution and the wall internal actions. The results allow also to draw some conclusions about the magnitude and the admissibility of the contribution of thermal loads, with reference to the wall global stability and structural safety.

2. Thermo-active diaphragm walls

2.1. Features of thermo-active diaphragm walls

In order to focus the analysis of thermo-active reinforced concrete diaphragm walls, or briefly energy walls, on the most specific features of their behaviour, a short review of similarities and differences with energy piles is presented here.

All the data collected from the experimental investigations on energy piles, together with the numerical and analytical predictions, confirm that the pile–soil interface resistance and the conditions at the pile head and toe, such as the presence of respectively an overstructure or a stiff substratum, represent constraints for the energy pile. In particular, they exert a restrain to the thermal expansion of the pile when heated and to the thermal contraction when cooled. These constraints lead to thermal induced stresses that act in addition to the stresses induced by the mechanical loads, and influence the final stress distribution.[34,36,50] More recently, the role of the soil–pile interface has been investigated in detail, accounting for the contribution of the thermo-mechanical behaviour of the interface itself,[51] the variations of the normal effective stresses induced by soil dilatant behaviour or by the concrete thermal contraction and expansion,[52,53] and the cyclic nature of the thermal load and its possible detrimental action on the shaft resistance, due to a large cumulated relative slip between soil and pile surface.[54,55]

It is worth remarking that the soil–pile interaction also depends on the thermo-hydro-mechanical behaviour of the surrounding soil, especially when saturated and fine grained. In this case, the difference in the thermal expansion coefficients of soil and water induces a short term increase of pore water pressures and a consequent long term consolidation process, leading to non-reversible volume variations. These are found to be contractions or dilations depending on the overconsolidation ratio.[56] Suitable non isothermal plasticity models were recently taken into account in refined numerical analyses of single energy piles and energy pile groups in clayey soils.[57,58]

In energy piles, significant changes were eventually pointed out in the mobilized shaft resistance and in the pile displacement and axial load and, although they are not expected to lead to detrimental consequences, they should be taken into consideration at the design stage.

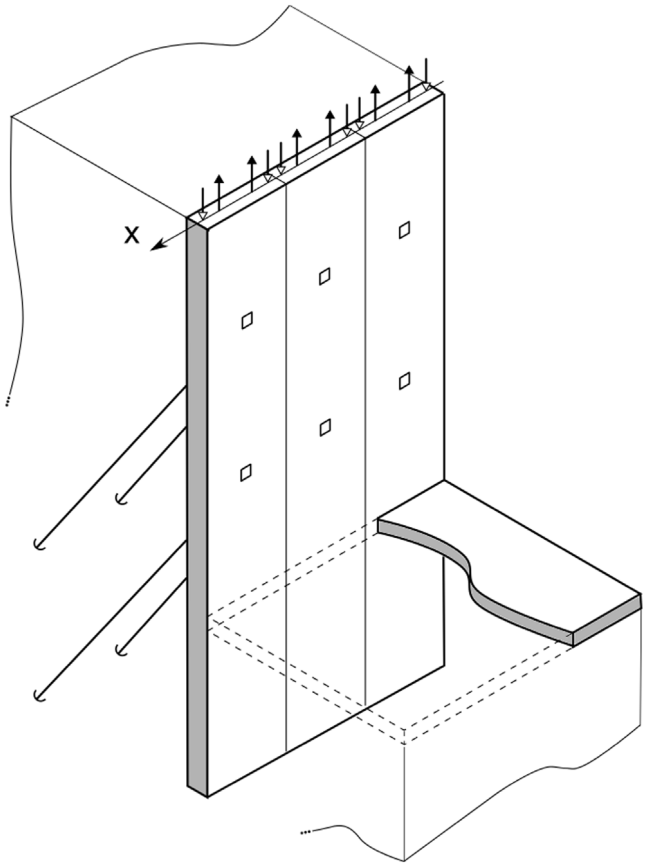

Fig. 1. Sketch of a three panels segment of an energy wall with anchors and base slab.

Thermally induced strains and stresses develop also in energy walls, but their effects are less predictable than in energy piles. Firstly, the wall has a greater complexity in terms of geometry (Fig. 1): the axisymmetric approximation is not applicable and various restraints could act on the wall from structural components such as anchors, struts, roof and base slabs, etc., that are absent in energy piles.

Secondly, the wall is fully embedded in the soil in its lowest part only, and the thermal boundary condition on the face exposed to the excavation could be uncertain. Basically, it depends on the use of the basement space, whether its temperature is controlled, it is ventilated and it has an open connection with the outside climate. The thermal condition on the exposed surface determines the direction and the magnitude of the heat flux, and the temperature differential in the wall width, thus playing a crucial role in both the energy performance and the mechanical behaviour.[49]

In addition, the length of the single panel is large enough to host a variety of different suitable layouts of the heat exchanger, with consequent different distributions of internal temperature induced by the heat transfer process. The influence of the pipe layout was dealt with also in the case of energy piles, in the frame of parameter sensitivity analysis and optimal design, and some layouts appear more efficient than others.[39,59–63] However, both operational constraints and the restriction in the pile section area allow for a limited choice and the U-shaped or W-shaped loops are eventually the most common choices. Diaphragm walls certainly offer broader possibilities of pipe layouts than piles, although some limits are imposed by the construction process, to avoid delays, and by quality requirements, to avoid potential causes of pipe damage or concrete casting defects.[15]

As to the energy performance, the heat transfer models developed for axisymmetric structures cannot be straightforwardly extended to energy walls and suitable models have to be developed, as discussed in the Introduction.[32,45] Also the interpretation of the Thermal Response Test, which is still under investigation even for energy piles,[64–67] requires further considerations in order to adapt the current models to the different geometry of the wall.

Due to difficulties inherent to the problem modelling and to the current exiguity of field monitoring data, mainly focused on the thermal performance and on the temperature gradients within the structure and the ground, the thermo-mechanical behaviour of energy walls has not yet been fully investigated.

The energy wall, as soil retaining structure, is basically subjected to horizontal earth pressures contrasted by its flexural response and by the possible presence of anchors and struts. The structural behaviour of the diaphragm wall is therefore entirely different from the one of piles; yet,

the thermal loads are expected to induce mainly an axial elongation/contraction effect similar to the one of piles.

Since the soil–wall interface shear resistance is not a key factor in the wall structural function, the possible detrimental action induced by cyclic thermal loads could be neglected, unless the diaphragm wall was used also with a load bearing function in the foundation system. Conversely, variations of lateral earth pressures induced by the soil contraction or dilatancy, or by the concrete thermal expansion and contraction, could be of interest.

The thermally induced elongation/contraction effects in the energy wall are generally not uniform along the wall longitudinal axis *x* (Fig. 1), for a given depth, due to a temperature gradient. In fact, the heat exchanger pipes might cover only part of the reinforcing cage within the single panel or, also, the distance between the downward directed and the upward directed portions of the pipe, that carry the fluid at different temperatures, might be not negligible. Therefore a significant temperature gradient exists along the *x* axis: alternate extension and contractions might occur and two vertical cross sections might be subjected to thermal loads of different magnitude. The different behaviour of the two sections and their mutual interaction lead to three-dimensional effects in the thermally induced stress–strain distribution and in the wall internal actions. This is an aspect probably less relevant in energy piles, nevertheless currently under consideration.[68]

A 3D approach to the analysis of the problem is therefore advisable, since the 2D plane strain approximation could be inaccurate. The recourse to a 3D domain is necessary also when the effects of a generic groundwater flow have to be taken into account and the simplified cases of a flow parallel or normal to the wall surface cannot be considered.

In the following, some of these aspects are discussed with reference to an energy wall, assembled with panels hosting two heat exchanger pipes each. The finite element analyses are based on a sequential thermo-mechanical coupling: a preliminary thermal analysis of the soil–structure system, subjected to seasonal atmospheric temperature conditions and to the seasonally alternate cooling/heating operation mode, permits to investigate the cyclic thermal working conditions and to assess the energy performance of the structure. The temperature variations under cyclic working conditions are then considered as thermal load in a thermo-mechanical analysis.

2.2. The retaining structure and the embedded heat exchangers

The energy wall problem discussed in the following was drawn from an existing reinforced concrete diaphragm wall equipped with heat exchangers, comprised in the foundation system of a six storeys residential building, with a three floors basement reaching the depth of 10 m below ground surface.

The building plan involved a roughly squared area of 40 m side, and the 10 m high excavation was supported by two pairs of facing diaphragm walls, with a height of 15 m and a thickness of 0.5 m. Also the basement floor

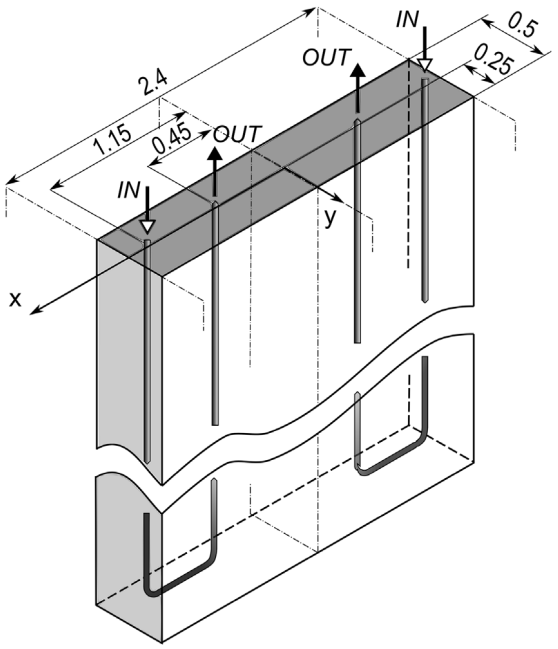

Fig. 2. Geometry and size of the single panel of the energy wall embedding two U-shaped heat exchangers (unit: m).

slab, in reinforced concrete, has a thickness of 0.5 m. An anchoring system, originally designed to improve the retaining capacity of the walls, was neglected in the analysis for the sake of simplicity. The presence of roof and intermediate slabs and of the overstructure was disregarded.

The diaphragm wall is formed by the connection of single panels of reinforced concrete, each of them is 2.4 m long and embeds two heat exchanger pipes (Fig. 2). Each pipe, made of high-density polyethylene plastic, has a 30 mm diameter. Each pipe loop occupies one third of the panel length, the central part being left free to allow for concrete casting without the risk of damaging the pipe. The pipes are fixed to the reinforcement cage before immersing it into the trench, but for the purpose of computations the loops were assumed laid in the longitudinal mid-section of the panel. This is recognized to be a major simplification of the problem. The loops reach a depth of 14.5 m within the panel and are assumed U-shaped, for a total length of about 30 m each. With this configuration the pipe inlets turn out to be very close each other, while the pipe outlets are more distant. As it will be outlined in the following, this layout was chosen to avoid all closeness between portions of the pipe which have very different temperatures. However, this configuration could be not the optimal one.

Considering the entire diaphragm wall, a series of parallel symmetry planes, vertical and normal to the plane of the wall, can be identified at a distance of 1.2 m from each other. Neglecting the effects of the end borders of the wall, the analysis of the three dimensional problem can be reduced to the 3D analysis of a 1.2 m wide slice corresponding to half of the single panel. Taking into account also the vertical symmetry plane through the centre of the excavation (right boundary of the domain), the final model is shown in Fig. 3.

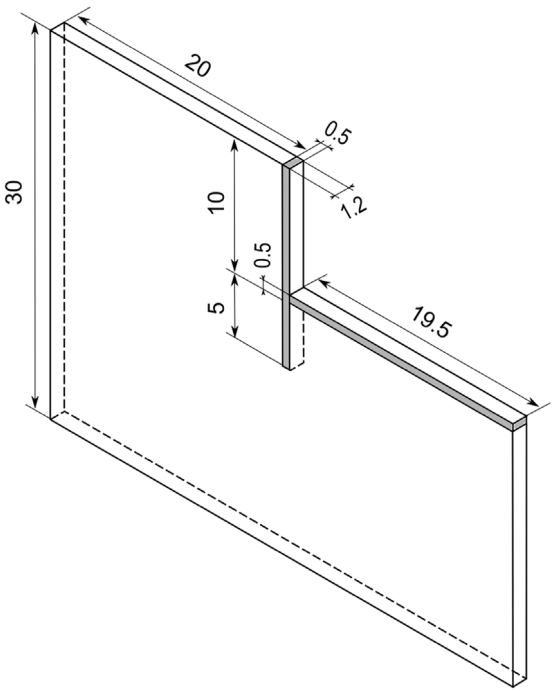

Fig. 3. Geometry and size of the three-dimensional domain, modelling half of the single panel of the energy wall (unit: m).

It is known that, in an energy geostructure of given geometry and for given thermal properties of the materials, the energy performance depends on the temperature inputs and on the characteristics of the fluid circulation, in particular the fluid velocity and the loop layout. The influence of the latter two parameters was preliminarily investigated with reference to a fully embedded ideal energy wall. A quarter of a single panel was modelled in three-dimensional finite element thermal analysis, where the heat transfer only was considered, neglecting all coupling with the hydro-mechanical behaviour.[69,70] The materials were assumed homogeneous and isotropic. Conduction was the only heat transfer process to be taken into account in the soil and in the reinforced concrete, while heat transfer by forced convection was modelled within the pipe by prescribing the constant fluid velocity and the temperature at the pipe inlet. Details on the governing equations are in the following Section 2.3. The summer cooling operating mode was considered, with an inlet fluid temperature of 30 °C and a constant velocity chosen in the range of 0.005 and 0.1 m/s. The far field ground temperature was 15 °C, while on the lateral sides of the model there are adiabatic conditions, being symmetry planes. Loop layouts n.1 to n.5 in Fig. 4 were considered and the results discussed assuming the layout n.1 as reference.

The heat flux Q [J/s] transferred by the circulating fluid, that can be assumed as a significant variable for assessing the system efficiency, is expressed as:

$$Q = \dot{m}_w c_w (T_{in} - T_{out}) \tag{1}$$

where $\dot{m}_w$ is the mass flow rate [kg/s], c_w is the fluid specific heat capacity [J/kg K] and T_{in}, T_{out} are respectively the fluid temperatures [K] at the loop inlet and outlet.

According to Eq. (1), for a given loop layout a high heat flux Q is obtained either for a high mass flow rate, i.e. a high fluid velocity, or for a high difference in temperatures between inlet and outlet, which is conversely reached when the fluid has a low velocity. As a consequence an optimal value of fluid velocity exists that leads to a maximum heat flux. Fig. 5 shows the dependence of the heat flux on the fluid velocity for the various layouts and the existence of the optimal value. Choosing the solution which optimizes the heat flux for all the layouts (i.e. $v = 0.01$ m/s), the performances of the 5 cases are compared in Fig. 6, showing that the efficiency in terms of heat flux depends on the loop layout, rather than on its length. In fact, configurations n.2 and n.3, although characterized by a long loop (70% more than the length of reference), are not associated with a high heat transfer, while the configuration n.5, despite only a 25% additional length, almost doubles the heat flux.

These results and the contour plots of the calculated temperature fields[70] suggest that the optimal layout of the pipe is the one that avoids the occurrence of high temperature gradients between adjacent portions of the pipe itself, that is clearly the situation induced in configurations n.2 and n.3. This provision would facilitate a gradual temperature variation of the fluid, i.e. gradual natural cooling or heating, without inducing interference and unfavourable opposite effects such as respectively re-heating or re-cooling.

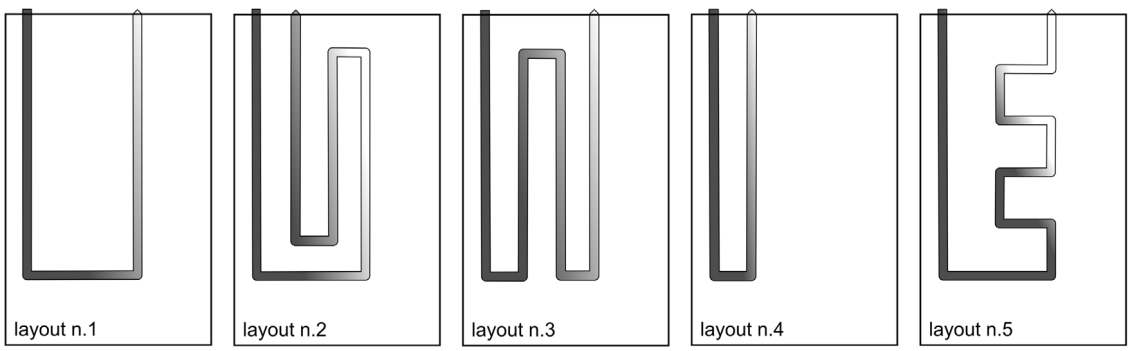

Fig. 4. Reference loop layout n.1 and alternative loop layouts n.2–n.5 of the exchanger pipe in the ideal energy wall panel.

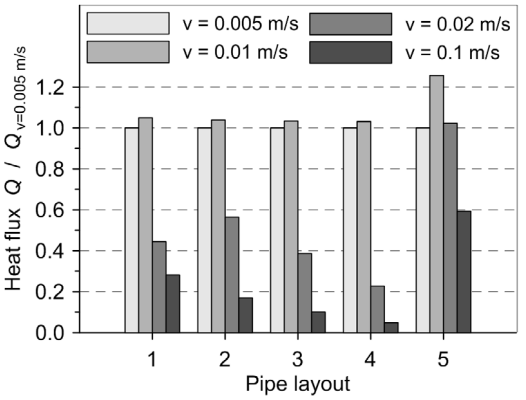

Fig. 5. Calculated heat flux for the layouts of Fig. 4 for different flow velocities, as percentage change with respect to the case $v = 0.005$ m/s.[70].

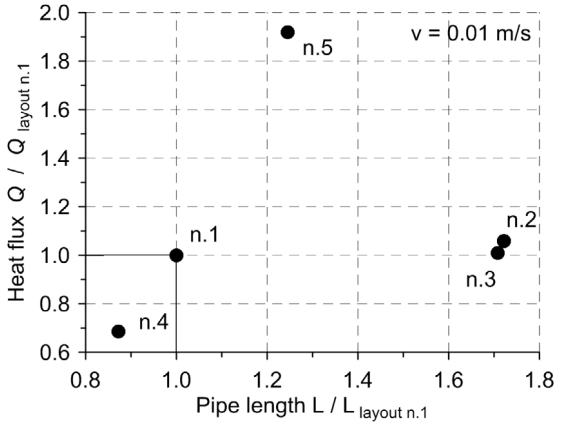

Fig. 6. Calculated heat flux for the layouts of Fig. 4 as a function of the pipe length, for $v = 0.01$ m/s, as percentage change with respect to the layout n.1.[70].

2.3. Governing laws and equations

The finite element analyses are based on a sequential thermo-mechanical coupling, and not on a fully coupled approach, since it can be assumed that a variation of temperature affects the stress–strain state of the bodies but not the opposite. Therefore, a preliminary thermal analysis is carried out, that leads to the determination of the variations in the temperature field, that turn out to be time-dependent due to the presence of time-dependent boundary conditions at the ground surface and the pipe inlet. Then, the temperature variations are applied as thermal loads in a following thermo-mechanical analysis. In Section 3.1 some considerations are addressed to the time-dependency and the steady state solution.

The thermal analysis is based on the laws governing the heat transfer in the various elements of the geothermal system and on the energy balance condition.[71] In the exchanger pipe the heat transfer occurs by conduction and forced convection, in the reinforced concrete elements by conduction and in the soil mass by conduction and convection, in the case there is a groundwater flow. Heat transfer by radiation and by phase change can be neglected in this kind of applications.

The physical and thermal properties of the soil mass, assumed as a saturated porous medium, are calculated here as weighted arithmetic means of the properties of the single phases, where the weights are the volume fractions.[25] Under this assumption, the equivalent homogeneous material has mass density ρ [kg/m^3], heat capacity ρc [J/m^3 K] and thermal conductivity $\underline{k}$ [J/(sm K)] respectively given by:

$$\begin{aligned} \rho &= (1-n)\,\rho_s + n\rho_w \\ \rho c &= (1-n)\,\rho_s c_s + n\rho_w c_w \\ \underline{k} &= (1-n)\,\underline{k}_s + n\underline{k}_w \end{aligned} \tag{2}$$

where subscripts w and s refer to the water and solid phases and n is the medium porosity, i.e. the water volume fraction in the case of full saturation.

In the general case of a porous medium saturated with a flowing incompressible fluid, the energy balance establishes that the rate of energy stored in the unit time and unit volume is equal to the sum of the heat flux per unit area $\underline{q}(\underline{x}, t)$ [J/(sm^2)] flowing into the volume partly by conduction ($\underline{q}_{cd}$) and partly by convection ($\underline{q}_{cv}$) in the unit time, and the heat $G(\underline{x}, t)$ [J/(sm^3)] supplied by an external source in the unit time and unit volume. In orthogonal coordinates, considering a unit volume having average mass density ρ, constant specific heat capacity c [J/kg K] and temperature $T(\underline{x}, t)$ [K], the energy balance is written as:

$$\rho c \frac{\partial T}{\partial t} = -\frac{\partial q_x}{\partial x} - \frac{\partial q_y}{\partial y} - \frac{\partial q_z}{\partial z} + G. \tag{3}$$

The heat transfer by conduction, assuming for the equivalent homogeneous material an isotropic thermal conductivity k, is governed by Fourier law:

$$\underline{q}_{cd} = -k\, grad\,(T)\,. \tag{4}$$

The heat transfer by convection depends on the characteristics of the groundwater flow (the fluid velocity $\underline{v}$ [m/s], its density ρ_w and its specific heat capacity c_w) according to the following equation, where T_0 is a reference temperature:

$$\underline{q}_{cv} = \rho_w c_w\, \underline{v}(T - T_0). \tag{5}$$

Substituting Eqs. (4) and (5) into Eq. (3) and considering a saturated and rigid porous body, for which the equation of fluid mass conservation holds true, the energy balance is written as:

$$\begin{aligned} &\rho c \frac{\partial T}{\partial t} + \rho_w c_w \left(v_x \frac{\partial T}{\partial x} + v_y \frac{\partial T}{\partial y} + v_z \frac{\partial T}{\partial z} \right) \\ &= k \left(\frac{\partial^2 T}{\partial x^2} + \frac{\partial^2 T}{\partial y^2} + \frac{\partial^2 T}{\partial z^2} \right) + G. \end{aligned} \tag{6}$$

In the present analyses, the additional conditions of negligible groundwater flow and absence of heat sources are introduced, so that Eq. (6) is simplified into the form:

$$\rho c \frac{\partial T}{\partial t} = k \left(\frac{\partial^2 T}{\partial x^2} + \frac{\partial^2 T}{\partial y^2} + \frac{\partial^2 T}{\partial z^2} \right). \tag{7}$$

This equation governs the heat transfer in both the soil mass and the concrete elements, once the pertaining thermal properties are assumed.

The heat flux in the heat exchanger pipe is modelled resorting to the conduction and convection equations, (4) and (5), where the thermal properties and the velocity pertain to the heat carrier fluid, namely k_f, $(\rho_f c_f)$ and $\underline{v}_f$, the latter assumed as an input constant value. In addition, the condition of fluid mass conservation holds true also for the heat carrier fluid, given the assumption of rigid pipe of constant section. For the elements modelling the pipe, the energy balance equation is therefore reduced to:

$$\rho_f c_f \left(\frac{\partial T}{\partial t} + v_{fx} \frac{\partial T}{\partial x} + v_{fy} \frac{\partial T}{\partial y} + v_{fz} \frac{\partial T}{\partial z} \right) = k_f \left(\frac{\partial^2 T}{\partial x^2} + \frac{\partial^2 T}{\partial y^2} + \frac{\partial^2 T}{\partial z^2} \right). \tag{8}$$

The initial condition, to obtain the solution $T(\underline{x}, t)$ from Eqs. (7) and (8), is represented by a temperature field $T(\underline{x}, 0)$ which has to be assigned. The boundary condition on convective surfaces, such as the inlet of the heat exchanger pipe, requires the input of the temperature and the velocity, or mass rate and density, of the fluid crossing the surface. The boundary conditions on conductive surfaces can consist in a prescribed temperature (Dirichlet condition), or in a prescribed temperature gradient, i.e. a heat flux crossing the unit area of the boundary surface (Neumann condition). The latter condition is used for instance to define adiabatic surfaces. Also a third type of boundary condition can be assigned on surfaces exposed to a fluid mass of known constant temperature, such as the ground surface (Newton's law of cooling). In the following analyses however, the simpler Dirichlet form is used, assuming that the air and the ground surface temperatures coincide.

The thermo-mechanical analysis is a conventional mechanical analysis of a saturated porous medium in drained conditions above groundwater table, i.e. with constant and negligible pore water pressures and uncoupled hydro-mechanical response, based on constitutive behaviours that account for isotropic linear thermo-elasticity and non-associated perfect plasticity in the soil mass, and for isotropic linear thermo-elasticity in the concrete elements. The elements modelled as heat exchanger in the previous thermal analysis, in this analysis are incorporated as concrete elements. The thermo-plasticity in the soil behaviour can be neglected, due to the coarse grained nature of the soil mass.[56]

The classic theory of thermo-elasticity in an isotropic medium has been considered, assuming that the temperature variation induces in the body only volume variations, i.e. that a volumetric effective stress rate $\dot{\sigma}'_{vol}$, a deviatoric stress rate $\dot{\sigma}_{dev}$ and a temperature rate $\dot{T}$ induce the volumetric and deviatoric components of the elastic strain rate:

$$\dot{\varepsilon}^e_{vol} = \frac{\dot{\sigma}'_{vol}}{K} + \alpha \dot{T}$$
$$\dot{\varepsilon}^e_{dev} = \frac{\dot{\sigma}_{dev}}{G} \tag{9}$$

where α, K and G are respectively the thermal expansion coefficient and the volumetric and tangential elastic moduli. The non-associated perfect plasticity, attributed to the soil mass only, adopts a Mohr–Coulomb yield function and a plastic potential function with hyperbolic shape in the meridional stress plane and smooth elliptic shape in the deviatoric stress plane.

The finite element analyses were performed with Abaqus 6.14 Software. For both thermal and thermo-mechanical analyses further details can be found in the Software Documentation.[72]

3. Thermal analyses

3.1. Numerical model and energy performance

The energy wall shown in Fig. 3, modelling half of the single panel of Fig. 2, was considered in a seasonally alternate operating mode, in sequentially coupled thermo-mechanical analyses. The preliminary thermal analysis allows to investigate the energy performance and to calculate the cyclic temperature variations induced in the wall and in the soil by the heat transfer process.

The physical and thermal properties of the saturated soil and the reinforced concrete, assumed as equivalent homogeneous materials, are calculated from relations (2) and are listed in Table 1. The subsoil consists of a saturated well graded silty sand, with porosity $n = 0.47$, in a hydrostatic regime. The volume ratio of reinforcement to concrete is equal to 1.5%; the thermal conductivity for reinforcements and concrete are equal to respectively 81 and 1.37 J/(sm K) and the specific heat to respectively 480 and 900 J/(kg K). Plain water, without additives, is used as heat carrier fluid. The thermal properties of the pipe are neglected.

The boundary condition at the pipe inlet (convective surface) consists of a prescribed constant fluid velocity (0.05 m/s) and of a fluid temperature $T_{in}(t)$ of yearly periodicity that depends on the operating mode of the geothermal system. Referring to a dual heating/cooling operating mode, the constant values of 2 °C and 30 °C are assumed respectively for the winter heating period, lasting 6 months from November to April, and for the summer cooling period, lasting 3 months from June to August. These extreme temperatures and extended periods are chosen in order to analyse the effects of severe thermal loads, likely upper and lower limits of the actual operating conditions. It must be remarked that a necessary refinement of the analysis would involve the modelling of the primary geothermal circuit coupled with a building energy dynamic simulation, so that for instance the thermal inputs can be more accurately defined.[73]

The thermal conditions on conductive surfaces consist of adiabatic conditions at the lateral boundaries and at the front and back faces of the domain, of uniform and constant temperatures at the base (15 °C) and at the internal sides of the excavation (18 °C), of a uniform and yearly cyclic temperature $T_s(t)$ at the ground surface, corresponding to the seasonally varying air temperatures (Fig. 7). The latter are provided by ARPA-Lombardia (Environmental Protection Regional Agency, Lombardia Region, Italy), as

Table 1
Physical and thermal properties.

	Density ρ (kg/m^3)	Thermal conductivity k (J/(sm K))	Specific heat c (J/(kg K))
Water/heat carrier fluid	1000	0.57	4186
Solid grains	2750	3.6	820
Saturated soil	1930	2.2	1642
Reinforced concrete	2500	2.6	880

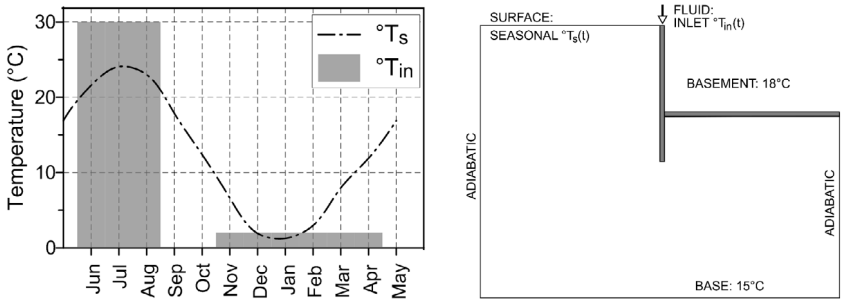

Fig. 7. Yearly seasonal variation of temperatures at the ground surface (dashed line) and at the inlet of the heat exchanger pipe (grey areas) and thermal conditions on the domain boundary.

average values over an 11 year time span (2001–2011) at a specific site in North-Western Italy, and reasonably confirm the customary assumption of sinusoidal variation of the atmospheric temperatures.[74]

The initial condition of the temperature field is the one obtained as steady state solution of a heat transfer process that considers only the temperature variation at the ground surface $T_s(t)$, before operating the geothermal system, and it has the same yearly periodicity.

Once the initial temperature field is set, the additional thermal input $T_{in}(t)$, associated with the geothermal system, modifies the natural heat transfer process. The new transient phase ends when a new overall energy balance is reached yearly, between the heat stored in the summer period and extracted in the winter period, as a combination of inputs from the geothermal system and from the boundary conditions. The steady state soil temperature field, of yearly periodicity, is reached after a transient phase lasting about 6 years.

The natural thermal energy recharge that the groundwater flow would supply to the soil mass, even in the short term, is absent in this case and the soil mass by itself can naturally rely only on the amount of energy provided by the thermal sources at the far field and at the upper boundary. In absence of groundwater flow, the seasonally alternated operating mode contributes to the thermal energy recharge with alternate periods of heat injections and extractions, and it is necessary, from one season to the next, for preserving the energy efficiency in the long term by limiting the permanent thermal drift within the soil mass.

It is worth stressing that, in the energy balance, the thermal condition at the exposed surfaces (building basement) governs the heat flux in the upper part of the wall,[49] and thus greatly influences the energy performance and the steady state temperature field. In this analysis, a uniform and constant temperature was assumed to represent a temperature controlled space (a warehouse or cellar, moderately heated in winter and naturally cool in summer). Alternatively, the presence of a space connecting with the outside (for instance a car parking) would require a varying temperature that depends on the outside climate. To analyse this different configuration, further computations are currently under consideration, adopting a temperature variation similar to $T_s(t)$ but with a lower amplitude, such that the maximum (summer time) and the minimum (winter time) values are respectively 6 °C lower and higher than the maximum and minimum atmospheric values. The first results are showing a slightly higher heat flux in summer time and a much lower heat flux in winter time (data not shown). These results would infer a rather different balance between heat injection and extraction, thus influencing the energy performance.

This is assessed by calculating first the exchanged heat flux in Eq. (1) from the fluid temperature at the outlet $T_{out}(t)$, and then the energy exchanged per month and per unit area of the wall. According to Eq. (1) the heat flux and the exchanged energy are positive when there is a decrease in the fluid temperature, i.e. when the thermal energy is stored in the soil mass in the summer cooling period, and are conversely negative when the thermal energy is extracted in the winter heating period.

Figs. 8 and 9 report the variations of the temperature at the outlet and of the exchanged energy, in the first year and in the steady state regime. The fluid temperature at the outlet undergoes a variation with time, after the month in which the system is turned on, in cooling or heating mode, due to the short term effect of thermal energy storage or extraction within the soil mass (Fig. 8). This reflects in a loss of energy efficiency of the system from the first month of operation to the last, that for instance in the steady state regime is equal to 12.3% between November and April and to 13.8% between June and August (Fig. 9).

Looking at the 6 year transient phase, the variation of fluid temperature at the outlet undergoes a noticeable change in the summer period and a minor change in the winter period (Fig. 8). In both periods a decrease in temperature is observed, corresponding to an increase in heat flux in summer and a decrease in winter. These

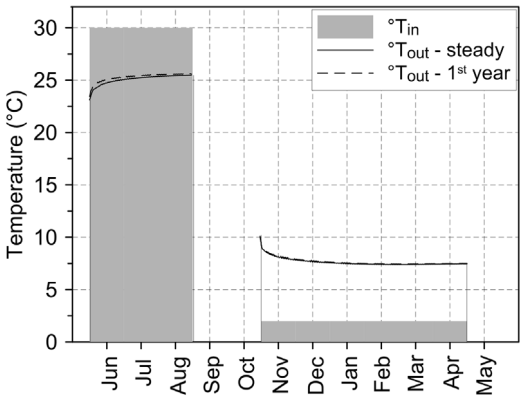

Fig. 8. Variations of temperatures at the pipe inlet and outlet in the first year (dashed lines) and in the steady state regime (solid lines).

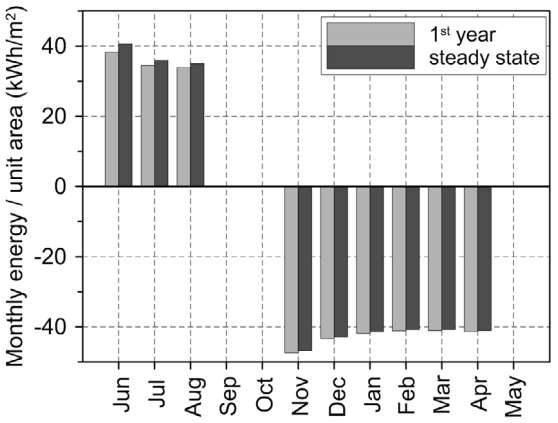

Fig. 9. Variations of monthly exchanged energy per unit area of the energy wall in the first year and in the steady state regime.

changes, occurring in the transient phase, are due to the large heat extraction in the winter period, that allows for an increase of heat injection potential in the next summer period, but causes at the same time a slight decrease of heat extraction potential in the next winter. Therefore, in the years the energy efficiency increases in the months of June and decreases in the months of November, until the new energy balance is reached in the steady state regime that starts approximately with the seventh year (Fig. 9). After this transient period, the energy efficiency has increased up to 6.2% in June, and decreased up to 1.2% in November, since the first year of operation.

3.2. Influence on the ground temperature field

The heat transfer process activated by the geothermal system induces a cyclic variation in the temperature field of the structures and of the soil mass, modifying the ordinary cyclic variation induced by the seasonal atmospheric temperatures.

At the end of the transient phase, when the soil–structure system has attained a new energy equilibrium over the year, permanent temperature variations in the soil mass can be found, customarily referred to as thermal drift. Even when freezing conditions of the subsoil are averted, the possible consequences of significant permanent temperature variations involve both environmental aspects, for instance the water solubility of salts and gaseous substances and the micro-organisms activity, and the energy performance of the geostructure, since permanent changes in the soil temperature affect the thermal storage capacity of the subsoil.

Analysing in Fig. 10 the transient phase in the soil mass, at various significant locations in the central section $x = 0.6$ m, different zones can be identified where the effects from the surface seasonal temperatures and from the geothermal system inputs are differently propagated. The points located very close to the wall are subjected to temperature variations basically governed by the heating/cooling phases (points A, B). In addition, the temperatures at points close to the wall and in the upper part of it markedly depend on the x position, since these points can be close to or far from the inlet portions of the exchanger pipe carrying the highest or lowest temperatures. For the points within a distance of about 2.5–3 m from the interface the dependence on the x coordinate has vanished, but the temperature variations are still governed by the phases of the geothermal system. At a larger distance from the wall, at shallow depth, the temperatures are conversely governed by the seasonal atmospheric variations (point C). At the same distance, but increasing depth, the cyclic behaviour is more limited and the effects of the transient phase become more evident in the years. This zone represents the large heat reservoir that undergoes a noticeable thermal drift of about 1 °C (points D–F). The same occurs beneath the wall, where the contribution of the geothermal system is clearly prevailing (point G). A last zone covers the positions where the boundary condition represented by the base slab prevails, limiting the cyclic effect of the geothermal system and the thermal drift (points H, I).

Analysing the steady state condition, the thermal variations induced by the geothermal system in the wall and in the nearby have highest values at the end of the cooling and heating periods, i.e. in August (highest temperature increase) and in April (highest temperature decrease). These two periods of the year are taken as reference in Fig. 11, that shows the contour lines of the undisturbed natural temperature field and of the temperature variations induced by the geothermal system, the latter with reference to two vertical cross sections: the closest to the pipe inlet ($x = 1.2$ m) and the most distant from it ($x = 0.0$ m). The difference between the temperature fields in these two sections brings evidence of the not negligible temperature gradient along the x direction, that affects the upper part of the wall and a narrow layer adjacent to the excavation. Fig. 11 also shows that the significant temperature variations are localized within 5–6 m from the wall surface in August, and 8–10 m in April. At the soil–wall interface, in the fully embedded part of the wall, the temperatures rise to 25.5 °C in August and drop to 6.2 °C in April, from the almost constant temperature of 16.8 °C in natural conditions. Finally, the thermal drift is revealed by the presence of a central zone where the temperature loss, with respect to the natural condition, is constant from April to August and is equal to about 1 °C.

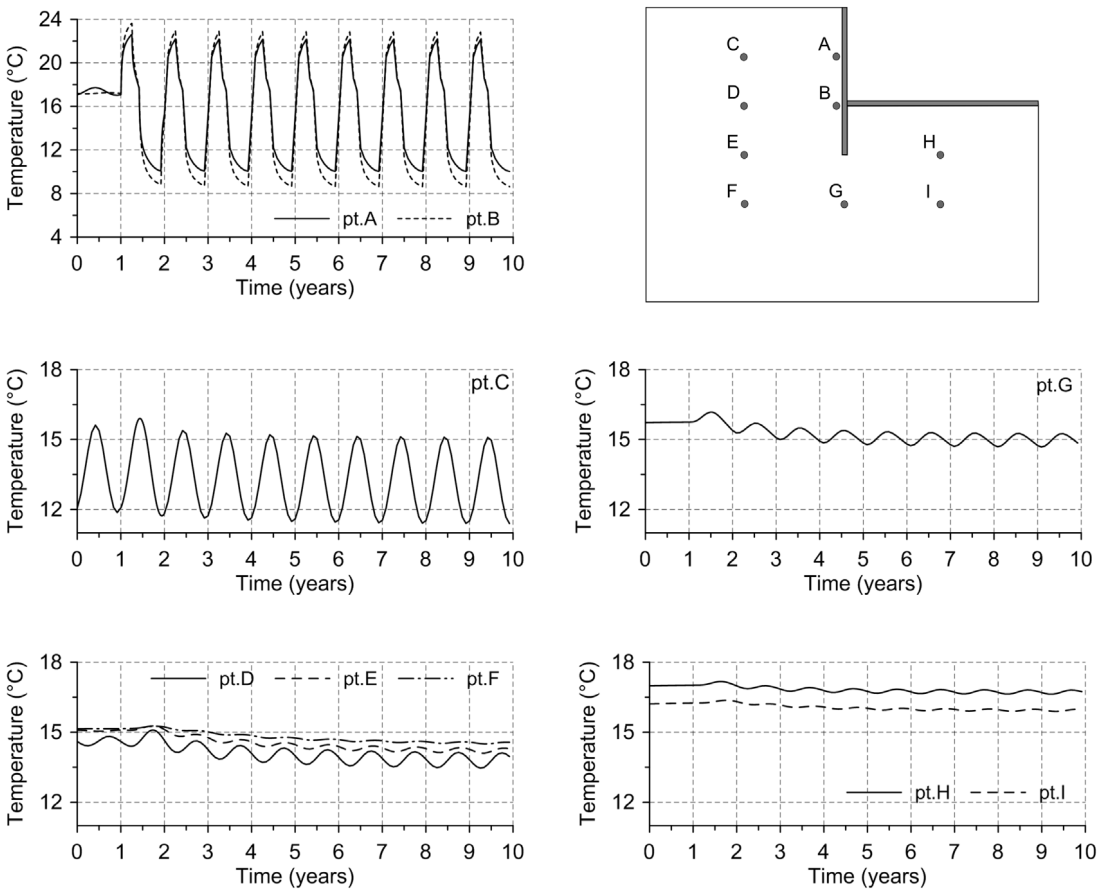

Fig. 10. Transient phase: variations of the temperature at significant positions in the soil mass, in section $x = 0.6$ m.

The effect of the thermal energy transfer from the wall to the soil is shown in Fig. 12, that represents the temperature variations, within the wall and the soil at its left side, along horizontal lines at depths 5 and 10.5 m. The profile of temperature within the wall (hatched area) remarks the influence of the fixed thermal boundary condition at the side of the excavation. In addition, the high rate of the heating process within the wall in the summer period is highlighted by the little difference in the temperatures between the first and the last month of the period (June and August). On the contrary the heat transfer within the soil mass occurs at a rate significantly lower, as shown by the large difference between the same curves referred to the soil mass. The same comment can be made about the rate of cooling in the winter period, comparing November with April conditions.

3.3. Influence on the temperatures within the energy wall

At the end of the transient phase, the temperature field within the energy wall ranges between two conditions of minimum and maximum values that are attained respectively in April and August. With reference to these two periods, Fig. 13 shows the temperature profile at the mid-section of the wall ($y = 0.0$), in three different vertical cross sections ($x = 0.0, 0.6, 1.2$ m). Section $x = 1.2$ m is located between the inlets of two exchanger pipes; therefore, the temperatures are here governed by the highest (30 °C in summer) or lowest (2 °C in winter) fluid temperatures and undergo the largest fluctuation in the year, ranging between rather uniform values of 4.6 °C in April and 28 °C in August. The sharp variation at the wall bottom is due to the fact that the exchanger pipe is embedded only up to the depth of 14.5 m.

Gradually moving away from this section (i.e. at $x = 0.6$ m), the temperature profile significantly changes and the influence of the inlet temperature decreases. At depths between 0 and 10 m the influence of the temperature of the basement prevails, and the temperature profiles tend to move to the constant value of 18 °C. Conversely, the fully embedded part of the wall (depths 10–15 m) is less influenced by the basement condition and is subjected to temperatures only slightly different from those calculated at section $x = 1.2$ m.

The section that is less influenced by the fluid temperature because most distant from the inlets ($x = 0.0$) undergoes the smallest temperature fluctuations in the year, in the ranges of 13.8–20.8 °C at the excavation side and of 6.2–25.7 °C in the embedded part of the wall.

It is also expected that the heat transfer process in the wall develops with heat flux magnitudes and directions that depend on the thermal boundary conditions. Considering the heat fluxes entering the wall from the soil side

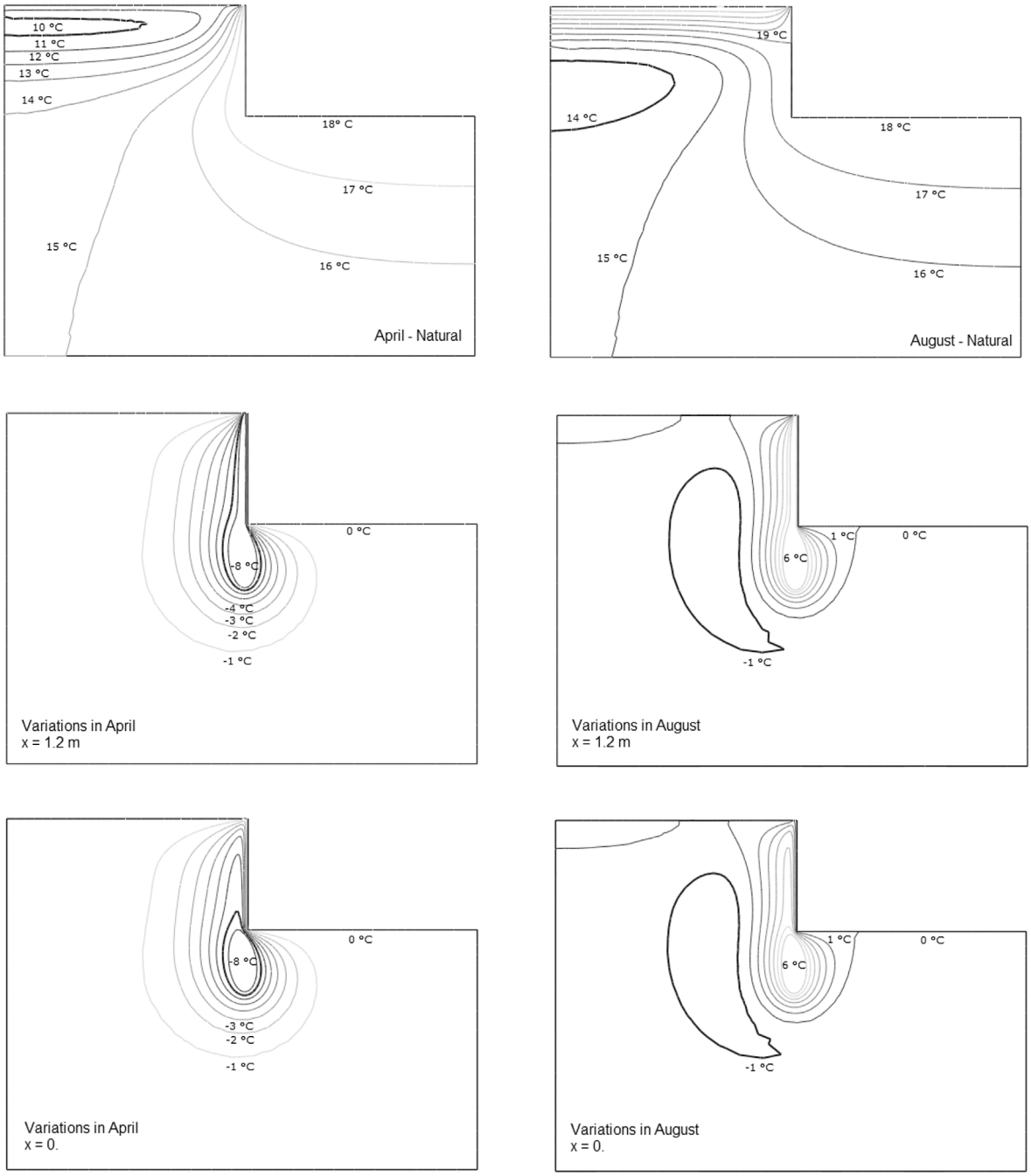

Fig. 11. Steady state regime in April (on the left) and August (on the right): absolute temperatures in natural undisturbed conditions (top) and temperature variations induced by the geothermal system in the vertical cross section $x = 1.2$ m (middle) and $x = 0.0$ (bottom).

and leaving the wall towards the excavation side, Fig. 14 reports the values calculated at the three cross sections, with reference to the same periods of April and August. Analysing the situation in April, the soil–wall surface is subjected to heat fluxes of limited magnitude, with respect to those at the exposed surface. As expected, the greatest absorption of heat is localized at section $x = 1.2$ m where, at depths of 0–10 m, it reaches average values of 37 W/m^2 entering from the soil and 146 W/m^2 entering from the excavation. It is interesting to note that section $x = 0$ is subjected to a negative flux at both surfaces, i.e. the heat is transferred from the basement to the soil through the wall. In the fully embedded part (depths 10–15 m), the wall absorbs heat from both surfaces with lower average values of flux, that drop to 11 W/m^2 from the left face and 14 W/m^2 from the right face. As regards the situation in August, similar comments can be drawn, with the only differences that in this case the heat flux tends to be in the opposite

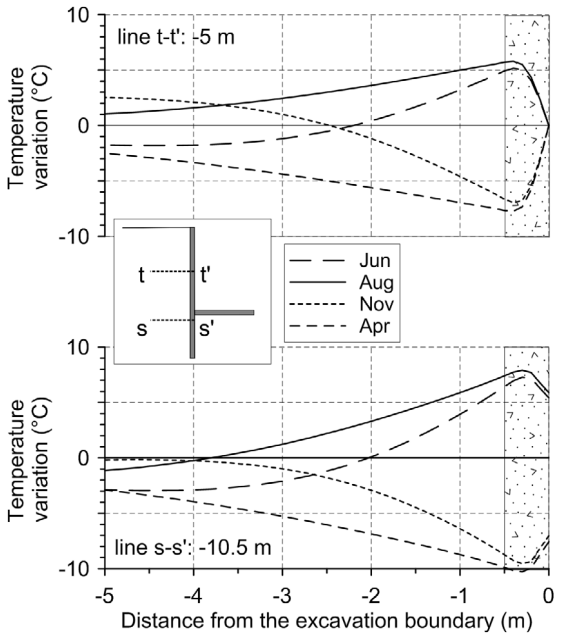

Fig. 12. Steady state regime in four periods of the year, in section $x = 0.6$ m, and depths 5 (line t–t′) and 10.5 m (line s–s′). The hatched area corresponds to the 0.5 m wide section of the energy wall.

direction and the heat exchange with the excavation is more limited, being the temperature difference between the inlet fluid and at the excavation surface more limited in August (+12 °C) than in April (−16 °C).

The comparison between the temperature profiles associated with the three different cross sections (Fig. 13) confirms the occurrence of a temperature gradient, along the x direction within the energy wall, which was shown also in Fig. 11. The gradient is rather significant in the upper part of the wall (average values of 7.7 °C/m in April and 6 °C/m in August) and decreases in the fully embedded part (average values of 1.3 °C/m in April and 1.8 °C/m in August). Under these conditions of internal temperature gradients, the consequent elongation (in the summer period) or contraction (in the winter period) is not uniformly distributed in the x direction, and consequent thermally induced internal stresses are expected to develop. In particular, in two different vertical cross sections different states of internal compressive or tensile vertical stress will show up, depending on respectively the greater or lower temperature variation developing in the two sections.

Finally it is worth remarking that a different temperature condition at the excavation side would influence not only the energy performance but also the internal stress/strain distribution.

4. Thermo-mechanical analyses

4.1. Numerical model and initial conditions

The assumptions about the mechanical constitutive behaviour for the soil mass and the reinforced concrete are briefly described in Section 2.3. It should be reminded that, although the silty component yields a not negligible cohesion, the soil was considered coarse grained, therefore the thermal effects on the mechanical behaviour were limited to a thermal elastic volumetric expansion and the hydro-mechanical coupling effects were neglected.

The mechanical parameters are listed in Table 2. For the soil mass, a stiffness increasing with depth was assumed. In a 12.5 cm thick layer of elements adjacent to the wall, lower shear strength and dilatancy values were considered, to represent a condition of altered soil–wall interface.

The thermo-mechanical analyses were performed on the three-dimensional model in Fig. 3, where the soil volume to be excavated was also modelled. The analyses include:

- a preliminary step for setting the initial geostatic stress state in oedometric conditions ($K_0 = 0.43$, for a given Poisson coefficient $\nu = 0.3$);
- the activation of the wall elements, following the customarily accepted "wished-in" diaphragm wall construction simulation (i.e. the construction induces no effects on the stress/strain state);

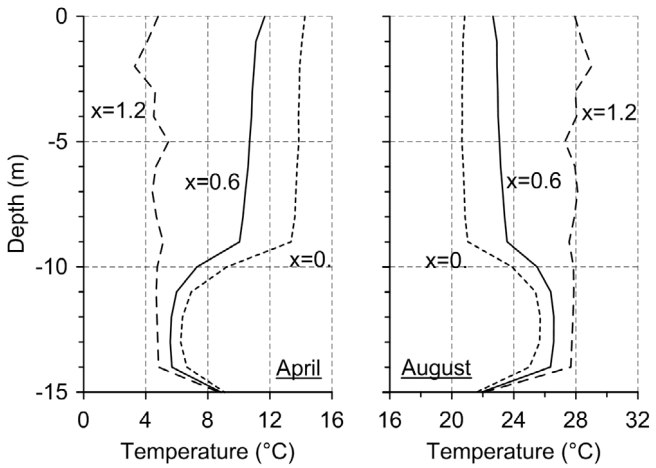

Fig. 13. Steady state regime in April (on the left) and August (on the right): temperature profile in the central section of the energy wall ($y = 0.0$) at three different vertical cross sections ($x = 0.0, 0.6, 1.2$ m).

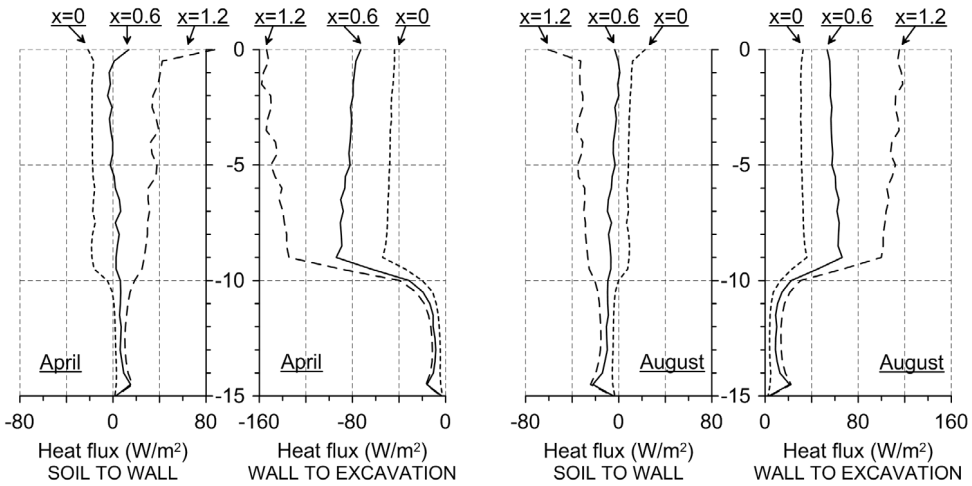

Fig. 14. Steady state regime in April (on the left) and August (on the right): heat flux through the wall faces at three different vertical cross sections, $x = 0.0, 0.6, 1.2$ m (positive in the y direction).

Table 2
Thermo-mechanical properties.

	Young modulus E MPa	Poisson coeff. ν –	Cohesion c kPa	Friction angle ϕ °	Dilatancy angle ψ °	Thermal expansion α 1/°C
Saturated soil	80–120	0.3	10	32	15	10^{-5}
Soil–wall interface	80–100	0.3	1	22.6	5	10^{-5}
Reinforced concrete	30 000	0.2	–	–	–	$1.5\ 10^{-5}$

- the removal of soil elements, simulating the excavation by layers of 0.5 m thickness;
- the activation of the floor slab elements.

Up to this step an ordinary diaphragm wall at working condition is modelled, eventually characterized by a time independent stress/strain field $\underline{\sigma}_0(\underline{x})$, $\underline{\varepsilon}_0(\underline{x})$ and in absence of a temperature field (standard mechanical solution). Then, the next steps include:

- the definition of an initial temperature field $T_0(\underline{x}, t_0)$, used as reference for the temperature variations and calculated from the steady state solution of the thermal analysis in undisturbed natural conditions (only atmospheric temperature conditions);
- the application of temperature variations $\Delta T(\underline{x}, t)$ as thermal loads, calculated as difference between the chosen initial $T_0(\underline{x}, t_0)$ and the current temperature field $T(\underline{x}, t)$ resulting from operating the geothermal system.

As regards the latter step, a preliminary analysis considered a time independent temperature variation $\Delta T(\underline{x}, t_{\text{aug}})$ by fixing the time associated with the highest temperature increase ($t = t_0 = t_{\text{aug}} =$ end of August), i.e. with the most demanding working condition for the energy wall over the year.[75]

The analysis reported in the following, on the contrary, assumed a time dependent temperature variation $\Delta T(\underline{x}, t)$ that covered a yearly cycle of geothermal system operation starting with time t_0, with the purpose to get insights into the entire range of variation of the significant stress/strain variables $\underline{\sigma}(\underline{x}, t)$, $\underline{\varepsilon}(\underline{x}, t)$. In this analysis, the reference initial condition $T_0(\underline{x}, t_0)$ was associated with time $t_0 =$ $t_{\text{may}} =$ end of May, assuming that the first operating mode of the geothermal system is the summer cooling.[76]

It is worth remarking that some preliminary thermo-mechanical analyses were carried out to investigate the influence of the natural atmospheric temperatures on the stress/strain field. In this case, the thermal loads are associated with the variations $\Delta T(\underline{x}, t)$ calculated as difference between the constant temperature field $T_0(\underline{x}, t_{\text{may}})$ and the time dependent field $T_0(\underline{x}, t)$ in the steady state regime. The results show that the natural atmospheric temperatures induce not significant variations in the stress/strain field with respect to the standard mechanical solution $\underline{\sigma}_0(\underline{x})$, $\underline{\varepsilon}_0(\underline{x})$. At this stage, in fact, the thermally induced stresses depend basically only on the different thermal expansion coefficients of soil and concrete, since the temperature field induced by the atmospheric conditions is rather smooth and the gradients between the ground and the wall are not significant. Conversely, when the heat exchanger is activated, the temperature variations will be higher and faster within the wall with respect to the soil, and this effect will eventually lead to very important thermally induced variations in the stress/strain field. This finding is however not always confirmed in the literature,[49] perhaps also due to different definitions about the reference temperature $T_0(\underline{x}, t)$ on which basis the variations $\Delta T(\underline{x}, t)$ are calculated. This aspect deserves further investigation.

4.2. Soil–structure interaction

The results reported in the following refer to the thermo-mechanical analysis that accounts for temperature

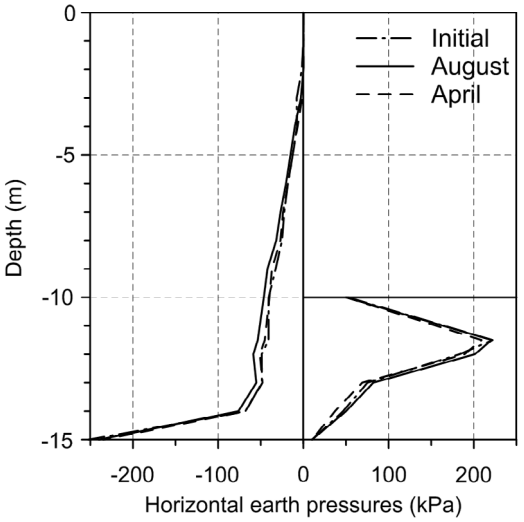

Fig. 15. Horizontal earth pressures on the wall at the end of the cooling (August) and heating (April) operating modes ($x = 1.2$ m).

variations $\Delta T(\underline{x}, t)$ covering the first year of operation of the geothermal system, starting with a summer cooling period and assuming the end of May for the reference temperature field $T_0(\underline{x}, t_{may})$.

The horizontal earth pressures are influenced by the thermal expansion of the materials and, therefore, vary over the year between lowest and highest values reached in the periods associated with lowest and highest temperatures in the wall and in the soil mass close to it, i.e. respectively in April and August. Despite the significant differences in temperature between different vertical cross sections (Fig. 13) the variations of horizontal earth pressures along the x axis are very limited.

Fig. 15 reports the pressure distributions on the two faces of the wall, in the vertical cross section $x = 1.2$ m. The maximum increases of pressure between April and August, occurring at the depth of 12 m, are equal to about 10% in the active zone and 7% in the passive zone. In comparison with the pressures in undisturbed natural conditions, these distributions represent minor variations, that can be considered quantitatively not relevant and do not affect the structural equilibrium.

The deformed configuration of the wall undergoes variations that can be analysed with reference to the vertical and horizontal components of displacements of the same section $x = 1.2$ m, since the difference between the deformed configuration at different vertical cross sections is never greater than 10^{-5} m. Fig. 16 shows the vertical component in the same two periods of the year compared with the one obtained in absence of geothermal system at the time t_{may}. The first summer period induces a thermal elongation that corresponds to upward movements in the upper part of the wall and downward movements in the lower part, while during the winter period the thermal contraction induces the opposite movement. The so called null section, i.e. the section not subjected to a vertical movement between summer and winter periods, is located in the fully embedded part of the wall, which is the part where the wall experiences the highest confinement. The maximum fluctuation of the vertical displacement occurs at the wall top, with an increase (in August) or a decrease (in April) equal to about 13% of the value in initial undisturbed conditions. In terms of absolute values, the maximum fluctuation is of the order of 2 mm. These vertical displacements will reflect in the wall internal axial force and bending moment, as shown in Section 4.3.

Lower percent values are calculated for the horizontal component of the wall displacement, shown in Fig. 17. Generally, in the summer period the wall moves towards the excavation in the upper part and in the opposite direction in the lower fully embedded part. The wall top undergoes the maximum displacement increase, equal to 7.0 mm, i.e. +8% of the initial value. In the winter period the behaviour is rather different from what observed for the vertical component of displacements: there is no substantial reversal of the displacements and in the upper part the contraction due to the low temperatures induces a further increase of positive displacements and an inversion of the curvature. The influence of the base slab at depth 10 m in constraining the horizontal displacement is also clear. The variation between August and April is shown also in Fig. 18, where the difference between the deformed

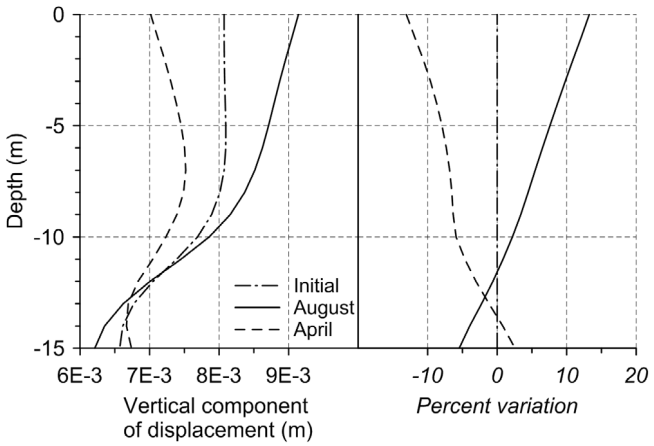

Fig. 16. Vertical component of the wall displacement in initial configuration (atmospheric temperatures) and at the end of cooling (August) and heating (April) operating modes, and percent variation with respect to the initial configuration ($x = 1.2$ m).

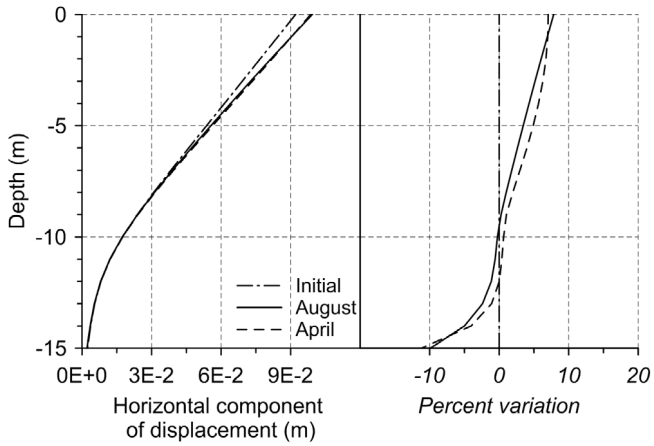

Fig. 17. Horizontal component of the wall displacement in initial configuration (atmospheric temperatures) and at the end of cooling (August) and heating (April) operating modes, and percent variation with respect to the initial configuration ($x = 1.2$ m).

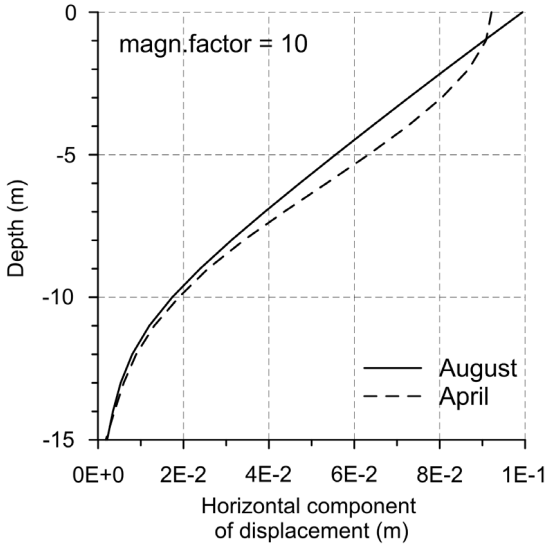

Fig. 18. Magnified deformed configuration in the horizontal direction at the end of the heating operating mode (April), with respect to the end of August ($x = 1.2$ m).

configurations has been magnified by a factor of 10 for the sake of clarity.

From these calculated values, the thermal effects seem to be acceptable in terms of geotechnical safety, at least in the first year of operation. The effects due to the possible cumulated displacements in the next years of operations are currently under investigation.

4.3. Structural response of the energy wall

The minor variations of wall displacements correspond to major thermally induced stresses that lead to major variations in the wall internal actions. In addition, the temperature gradient arising in the x direction (Fig. 13), that does not induce significant differences in the displacement field in the different sections, conversely induces in the internal actions a remarkable gradient in the same x direction.

The internal actions considered in the following are axial forces and bending moments per unit length of the wall in the x direction. They were calculated, at given sections $\bar{x}$, as the integrals along the y axis of respectively the axial stresses $\sigma_z(\bar{x}, y, z)$ and the moment of the axial stresses with respect to the centre line of the wall. Accounting for a wall of width h (0.5 m) and introducing the distance to the centre line as $d_{cl}(y)$, the two equations are:

$$F(\bar{x}, z) = \int_{-h/2}^{h/2} [\sigma_z(\bar{x}, y, z)]\, dy \tag{10}$$

$$M(\bar{x}, z) = \int_{-h/2}^{h/2} [\sigma_z(\bar{x}, y, z) \cdot d_{cl}(y)]\, dy \tag{11}$$

with units, respectively, kN/m and kNm/m. The sections $\bar{x} = 0.0$, 0.6, 1.2 m were chosen as the most meaningful for the following discussion.

Fig. 19 reports the internal axial force per unit length under undisturbed natural conditions and during the first year of operation of the geothermal system, in particular at four different time instants. As expected, the section closest to the heat exchanger inlet ($x = 1.2$ m) undergoes an increase in compressive axial force in the summer period and a decrease of it in the winter period, till the occurrence of even a tensile axial force, due to the restraints that limit respectively its thermal expansion when heated and contraction when cooled. These restraints are exerted by the soil at the wall faces, which has a lower thermal expansion coefficient and is subjected to lower temperature variations (Fig. 12), and by the adjacent sections of the wall itself which are not subjected to the same temperature variations (Fig. 13). The latter aspect, i.e. the interaction between adjacent sections, leads to a concurrent and opposite effect in the sections less influenced by the temperature variation (for instance the section $x = 0.0$ in Fig. 19), where a tensile (summer period) or compressive (winter period) axial force was calculated. The intermediate section ($x = 0.6$ m) shows an intermediate behaviour and is subjected to more limited variations of the axial force.

It can be also observed that, while the last months of each operating phase (August and April) are the time

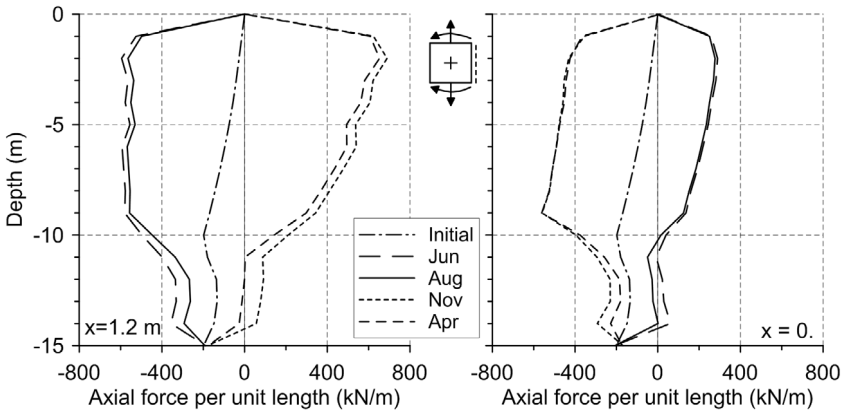

Fig. 19. Axial force per unit length in four periods of the year and two vertical cross sections: $x = 1.2$ m (left), $x = 0.0$ (right), with respect to the initial undisturbed condition.

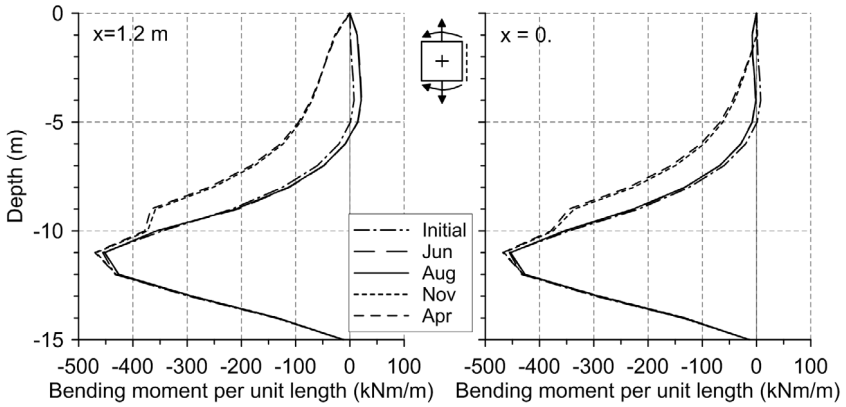

Fig. 20. Bending moment per unit length in four periods of the year and two vertical cross sections: $x = 1.2$ m (left), $x = 0.0$ (right), with respect to the initial undisturbed condition.

instants associated with the greatest temperature variations within the wall, the first months (respectively June and November) are the time instants associated with the highest axial force variations. This is due to the process of heat transfer that occurs in the soil at a lower rate than in the wall (Fig. 12): the fast thermal energy diffusion within the concrete element leads to the highest thermally induced stresses in the very first month of operation because the heat transfer has not yet involved the adjacent soil mass, that therefore offers the highest restraint to the wall free expansion or contraction. Slowly with time, the soil mass is also subjected to temperature variations, i.e. to thermal expansions or contractions, that are consistent with those of the wall and partially release the thermally induced stresses within it. This effect is more evident in the fully embedded part, where the wall is subjected to the confinement exerted by the soil on two sides. Similar findings were discussed with reference to pile groups, where the effects of the delayed heat transfer from the heated pile to the non-heated piles and to the foundation were observed. Alternate conditions of tensile/compressive states of stress among different piles were also reported.[77]

The variations induced in the bending moment are shown in Fig. 20. They can be justified by analysing the variations in the shear stresses at the soil–wall interface, that in turn depend on the relative movement between the soil and the wall during the periods of temperature increase (summer) or decrease (winter). Looking at the upper portion of the wall, at the side of the excavation (up to a 10 m depth) and in section $x = 1.2$ m, in the summer case the vertical movement is directed upwards (Fig. 16) and in the wall is larger than in the soil due to a larger thermal expansion coefficient, therefore the shear stresses on the wall face are directed downwards and lead to an increase of positive bending moment. In the winter case, the wall contraction corresponds to vertical movements directed downwards and still in the wall larger than in the soil. Therefore in this case the shear stresses on the wall face are directed upwards and lead to an increase of negative bending moments.

The bending moment variation calculated in section $x = 0.0$ is opposite to the one observed in section $x = 1.2$ m in the summer period. This result is justified on the basis of the interaction between adjacent sections of the wall, consistently with what observed in the case of axial force. In the winter period the bending moment is negative also in section $x = 0.0$, but the values are lower than in section $x = 1.2$ m. The interaction between adjacent sections is in this case revealed by the different magnitudes of the bending moments.

The contribution of the base slab in limiting these variations is evident in Fig. 20, and the bending moments in the fully embedded part of the wall, including the maximum value at depth 11 m, are almost unaffected by the heat transfer process.

Also the difference between the conditions at the first and the last month of operation in the bending moment distribution is less evident than in the axial force distribution.

As a conclusion, the thermal effects appear relevant in terms of variations of internal actions. From a structural point of view the values attained by the variables here considered during the heating and cooling periods in the first year of operation are not detrimental to the safety of the diaphragm wall. Nevertheless they highlight that the structure is subjected to additional stresses that cannot be neglected at the design stage.

It is also worth remarking that a more refined analysis should include the presence of an overstructure and of possible additional connected structures that would highly influence the internal stress distribution through additional displacement constraints and mechanical loads.

5. Conclusions

The reinforced concrete diaphragm walls have proved to be effective energy geostructures for the exploitation of the near surface geothermal energy. After assessing the behaviour of an energy wall from the perspective of both the geothermal energy exploitation and the short and long term influence on the soil temperatures by three-dimensional thermal analyses, its geotechnical and structural response was evaluated by sequentially coupled thermo-mechanical analyses, applying the time dependent thermal loads that correspond to a one year cycle of heating/cooling operation. The effects of the heat transfer process have been discussed in terms of soil–structure interaction (wall deformed configuration and earth pressures) and structural internal actions (axial forces and bending moments).

Simplifying hypotheses, that should be removed in a more refined analysis, include the absence of anchors and connected structures, the position and layout of the pipe, a thermal input characterized by constant values of fluid temperature at the pipe inlet over the heating/cooling periods, the constant temperature condition within the basement, and the absence of a groundwater flow.

From an energetic point of view, the following conclusions can be drawn:

- The energy wall takes advantage of a large surface extension for the heat transfer, and a proper pipe layout, combined with the prescribed fluid velocity, can optimize the energy performance.
- In the calculations, a correct description of the thermal boundary conditions is necessary, in particular at the side and base of the excavation, for the accurate evaluation of the heat fluxes and the consequent energy performance. Moreover, the heat transfer is generally not uniform in the longitudinal plane, but depends on the pipe layout.
- A correct description of the thermal input from the secondary circuit is also necessary. The most refined analysis would require modelling the primary circuit coupled with a building energy dynamic simulation.
- Finally, although the energy wall is usually limited to a shallow depth, the groundwater flow may be not negligible and have a remarkable influence on the heat storage potential within the soil mass and consequent energy performance.

All factors influencing the heat transfer process affect the temperature variations within the soils and the structure and, as a consequence, affect the mechanical response of the energy wall. Besides this, the main conclusions referred to the thermo-mechanical aspects of the problem are:

- The thermally induced effects on the structure are not negligible and can be observed partly as additional displacements, partly as variations of the internal actions. The temperature gradient arising in the longitudinal plane induces different behaviours in different adjacent vertical sections, that mutually interact restraining each other's thermal elongation or contraction. A three-dimensional model is therefore more accurate than the conventional plane strain model.
- The magnitude of the thermal effects depends also on the level of constraints the structure is subjected to. Therefore an accurate modelling of the geometry, including the connected structures, is important.
- Although the effects seem to be limited to a level that the geostructure could cope with, nevertheless a thermo-mechanical analysis at the design stage proves to be advisable, in order to highlight and quantify possible situations of unexpected overstress conditions for the diaphragm wall and the connected structures.

Further developments of the analyses are currently involving a more realistic description of the geometry and of the thermal inputs, and the calibration of the numerical model based on site monitoring data. The issues of the cyclic effect and of the long term mechanical response assessed over more years of operation will be also addressed, in order to highlight possible situations of cumulated displacements and of progressive damage, both within the structure and at the soil–wall interface.

Acknowledgements

The Authors acknowledge the support of COST Action TU1405 GABI (Geothermal Applications for Buildings and Infrastructures) and the inspiring discussions arisen during the Meetings.

References

[1] International Energy Agency. *Key World Energy Statistics 2014*. Paris: OECD/IEA; 2014:www.iea.org.
[2] Lund JW, Freeston DH, Boyd TL. Direct application of geothermal energy 2010 worldwide review. *Geothermics*. 2011;40:159–180.
[3] Pérez-Lombard L, Ortiz J, Pout C. A review on buildings energy consumption information. *Energy Build*. 2008;40:394–398.

[4] RHC-Platform. Strategic research priorities for renewable heating & cooling cross-cutting technology. European Technology Platform on Renewable Heating & Cooling, Brussels 2012. (www.rhc-platform.org).

[5] European Parliament and Council. Directive 2010/31/EU on the energy performance of buildings. *Off J Eur Union L*. 2010;153/13.

[6] Olgun CG, Bowers GA. Ground-source bridge deck de-icing systems using energy foundations. In: Laloui L, Di Donna A, eds. *Energy Geostructures*. ISTE and John Wiley & Sons; 2013:211–225, (Chapter 11).

[7] Dupray F, Li C, Laloui L. Heat-exchanger piles for the de-icing of bridges. *Acta Geotech*. 2014;9:413–423.

[8] Preene M, Powrie W. Ground energy systems: from analysis to geotechnical design. *Géotechnique*. 2009;59(3):261–271.

[9] Bourne-Webb PJ, Amis T, Bernard J-B, Friedemann W, von der Hude N, Pralle N, Uotinen VM, Widerin B. Delivery of energy geostructures. In: Laloui L, Di Donna A, eds. *Energy Geostructures*. ISTE and John Wiley & Sons; 2013:229–264.

[10] Laloui L, Di Donna A. *Energy Geostructures*. ISTE and John Wiley & Sons; 2013.

[11] Brandl H. Energy foundations and other thermo-active ground structures. *Géotechnique*. 2006;56(2):81–122.

[12] Adam D, Markiewicz R. Energy from earth-coupled structures, foundations, tunnels and sewers. *Géotechnique*. 2009;59(3):229–236.

[13] Bourne-Webb PJ, Amatya B, Soga K, Amis T, Davidson C, Payne P. Energy pile test at Lambeth College, London: geotechnical and thermodynamic aspects of pile response to heat cycles. *Géotechnique*. 2009; 59(3):237–248.

[14] Hamada Y, Saitoh H, Nakamura M, Kubota H, Ochifuji K. Field performance of an energy pile system for space heating. *Energy Build*. 2007;39:517–524.

[15] Amis T, Robinson CAW, Wong S. Integrating geothermal loops into the diaphragm walls of the Knightsbridge Palace Hotel project. In *Proc. 11th DFI/EFFC Int. Conf. Geotechnical Challenges in Urban Regeneration, London*. 2010.

[16] Xia C, Sun M, Zhang G, Xiao S, Zou Y. Experimental study on geothermal heat exchangers buried in diaphragm walls. *Energy Build*. 2012;52:50–55.

[17] Frodl S, Franzius JN, Bartl T. Design and construction of the tunnel geothermal system in Jenbach. *Geomech Tunnelling*. 2010;3(5): 658–668.

[18] Nicholson DP, Chen Q, Pillai A, Chendorain M. Developments in thermal pile and thermal tunnel linings for city scale GSHP systems. In: *Proc. 38th Workshop Geothermal Reservoir Engineering*. Stanford (CA), USA: Stanford University; 2013: SGP-TR-198.

[19] Zhang G, Xia C, Yang Y, Sun M, Zou Y. Experimental study on the thermal performance of tunnel lining ground heat exchangers. *Energy Build*. 2014;77:149–157.

[20] Barla M, Di Donna A, Perino A. Application of energy tunnels to an urban environment. *Geothermics*. 2016;61:104–113.

[21] Mimouni T, Dupray F, Laloui L. Estimating the geothermal potential of heat-exchanger anchors on a cut-and-cover tunnel. *Geothermics*. 2014;51:380–387.

[22] Banks D. Site investigation (ground conditions/licences and permits). In: McCorry M, Jones GL, eds. *Geotrainet Training Manual for Designers of Shallow Geothermal Systems. Geotrainet*. Brussels: European Federation of Geologists; 2011:71–92, (Chapter 9) www.geotrainet.eu.

[23] Lualdi M. TRUE 3D Acquisition using GPR over small areas: A cost effective solution. In *Proc. 24th Symposium on the Application of Geophysics to Engineering and Environmental Problems 2011, SAGEEP, Charleston (SC), USA*. 2011, pp. 541–550.

[24] Lualdi M, Lombardi F. Utilities detection through the sum of orthogonal polarization in 3D georadar surveys. *Near Surf Geophys*. 2015;13(1):73–81.

[25] Rees SW, Adjali MH, Zhou Z, Davies M, Thomas HR. Ground heat transfer effects on the thermal performance of earth-contact structures. *Renewable Sustainable Energy Rev*. 2000;4(3):213–265.

[26] Beier RA, Smith MD, Spitler JD. Reference data sets for vertical borehole ground heat exchanger models and thermal response test analysis. *Geothermics*. 2011;40:78–85.

[27] Bourne-Webb P, da Costa Gonçalves R. On the exploitation of ground heat using transportation infrastructure. In *Proc. 3rd Int. Conf. on Transportation Geotechnics ICTG 2016. Procedia Engineering, Vol. 143*. 2016, pp. 1333–1340.

[28] Adjali MH, Davies M, Rees SW. A comparative study of design guide calculations and measured heat loss through the ground. *Build Environ*. 2004;39(11):1301–1311.

[29] Thomas HR, Rees SW. Measured and simulated heat transfer to foundation soils. *Géotechnique*. 2009;59(4):365–375.

[30] Angelotti A, Alberti L, La Licata I, Antelmi M. Energy performance and thermal impact of e Borehole Heat Exchanger in a sandy aquifer: influence of the groundwater velocity. *Energy Convers Manage*. 2014; 77:700–708.

[31] Suryatriyastuti ME, Mroueh H, Burlon S. Impact of transient heat diffusion of a thermoactive pile on the surrounding soil. In: Laloui L, Di Donna A, eds. *Energy Geostructures*. ISTE and John Wiley & Sons; 2013:193–209, (Chapter 10).

[32] Kürten S, Mottaghy D, Ziegler M. A new model for the description of the heat transfer for plane thermo-active geotechnical systems based on thermal resistances. *Acta Geotech*. 2015;10:219–229.

[33] Di Donna A, Barla M. The role of ground conditions on energy tunnels' heat exchange. *Environ Geotech*. 2016;3:214–224.

[34] Amatya BL, Soga K, Bourne-Webb PJ, Amis T, Laloui L. Thermo-mechanical behaviour of energy piles. *Géotechnique*. 2012;62(6): 503–519.

[35] Murphy KD, McCartney JS, Henry KS. Evaluation of thermo-mechanical and thermal behavior of full-scale energy foundations. *Acta Geotech*. 2015;10:179–195.

[36] Laloui L, Nuth M, Vulliet L. Experimental and numerical investigations of the behaviour of a heat exchanger pile. *Int J Numer Anal Methods Geomech*. 2006;30(8):763–781.

[37] Knellwolf C, Peron H, Laloui L. Geotechnical analysis of heat exchanger piles. *ASCE J Geotech Geoenviron Eng*. 2011;137(10): 890–902.

[38] Suryatriyastuti ME, Mroueh H, Burlon S. Understanding the temperature-induced mechanical behavior of energy pile foundations. *Renewable Sustainable Energy Rev*. 2012;16:3344–3354.

[39] Caulk R, Ghazanfari E, McCartney JS. Parametrization of a calibrated geothermal energy pile model. *Geomech Energy Environ*. 2016;5: 1–15.

[40] Kalantidou A, Tang AM, Pereira J-M, Hassen G. Preliminary study on the mechanical behaviour of heat exchanger pile in physical model. *Géotechnique*. 2012;62(11):1047–1051.

[41] Stewart MA, McCartney JS. Centrifuge modeling of soil-structure interaction in energy foundations. *ASCE J Geotech Geoenviron Eng*. 2014;140(4):04013044-1.11.

[42] Kramer CA, Ghasemi-Fare O, Basu P. Laboratory thermal performance tests on a model heat exchanger pile in sand. *Geotech Geol Eng*. 2015;33:253–271.

[43] Goode III JC, McCartney JS. Centrifuge modelling of end-restraint effects in energy foundations. *ASCE J Geotech Geoenviron Eng*. 2015; 141(8):04015034-1.13.

[44] Rotta Loria AF, Gunawan A, Shi C, Laloui L, Ng CWW. Numerical modelling of energy piles in saturated sand subjected to thermo-mechanical loads. *Geomech Energy Environ*. 2015;1:1–15.

[45] Sun M, Xia C, Zhang G. Heat transfer model and design method for geothermal heat exchange tubes in diaphragm walls. *Energy Build*. 2013;61:250–259.

[46] Unterberger W, Hofinger H, Grünstäudl T, Markiewicz R, Adam D. Utilization of tunnels as sources of ground heat and cooling – Practical applications in Austria. iC consulenten Ziviltechniker GesmbH Publications. 2014, pp. 1–6. (www.ic–group.org).

[47] Soga K, Rui Y, Nicholson D. Behaviour of a thermal wall installed in the tottenham court road station box. In *Proc. Crossrail Conference, Crossrail Ltd and Federation of Piling Specialists, City Hall, London*. 2015, pp. 112–119.

[48] Habert J, Burlon S. Modelling thermo-active diaphragm walls. In *Proc. 2nd EAGE Workshop on Geomechanics and Energy*. 2015, pp. 100–104.

[49] Bourne-Webb PJ, Bodas Freitas TM, da Costa Gonçalves RA. Thermal and mechanical aspects of the response of embedded retaining walls used as shallow geothermal heat exchangers. *Energy Build*. 2016; 125:130–141.

[50] Gashti EHN, Malaska M, Kujala K. Evaluation of thermo-mechanical behaviour of composite energy piles during heating/cooling operations. *Eng Struct*. 2014;75:363–373.

[51] Di Donna A, Ferrari A, Laloui L. Experimental investigations of the soil–concrete interface: physical mechanisms, cyclic mobilization, and behaviour at different temperatures. *Can Geotech J*. 2016;33: 659–672.

[52] Olgun CG, Ozudogru TY, Arson CF. Thermo-mechanical radial expansion of heat exchanger piles and possible effects on contact pressures at pile–soil interface. *Geotech Lett*. 2014;4(3):170–178.

[53] Ozudogru TY, Olgun CG, Arson CF. Analysis of friction induced thermo-mechanical stresses on a heat exchanger pile in isothermal soil. *Geotech Geol Eng*. 2015;33:357–371.

[54] Saggu R, Chakraborty T. Cyclic thermo–mechanical analysis of energy piles in sand. *Geotech Geol Eng*. 2015;33(2):321–342.

[55] Suryatriyastuti ME, Mroueh H, Burlon S. A load transfer approach for studying the cyclic behaviour of thermo-active piles. *Comput Geotech*. 2014;55:378–391.
[56] Cekerevac C, Laloui L. Experimental study of thermal effects on the mechanical behaviour of a clay. *Int J Numer Anal Methods Geomech*. 2004;28(3):209–228.
[57] Laloui L, Cekerevac C. Non isothermal plasticity model for cyclic behaviour of soils. *Int J Numer Anal Methods Geomech*. 2008;32(5): 437–460.
[58] Di Donna A, Laloui L. Numerical analysis of the geotechnical behaviour of energy piles. *Int J Numer Anal Methods Geomech*. 2015; 39:861–888.
[59] Zarrella A, De Carli M, Galgaro A. Thermal performance of two types of energy foundation pile: Helical pipe and triple U-tube. *Appl Therm Eng*. 2013;61:301–310.
[60] Batini N, Rotta Loria AF, Conti P, Testi D, Grassi W, Laloui L. Energy and geotechnical behaviour of energy piles for different design solutions. *Appl Therm Eng*. 2015;86:199–213.
[61] Cecinato F, Loveridge F. Influences on the thermal efficiency of energy piles. *Energy*. 2015;82:1021–1033.
[62] Loveridge F, Cecinato F. Thermal performance of thermoactive continuous flight auger piles. *Environ Geotech*. 2016;3:265–279.
[63] Kaltreider C, Krarti M, McCartney J. Heat transfer analysis of thermo-active foundations. *Energy Build*. 2015;86:492–501.
[64] Park H, Lee S-R, Yoon S, Choi J-C. Evaluation of thermal response and performance of PHC energy pile: Field experiments and numerical simulation. *Appl Energy*. 2013;103:12–24.
[65] Li M, Lai ACK. Review of analytical models for heat transfer by vertical ground heat exchangers (GHEs): A perspective of time and space scales. *Appl Energy*. 2015;151: 198–191.
[66] Franco A, Moffat R, Toledo M, Herrera P. Numerical sensitivity analysis of thermal response tests (TRT) in energy piles. *Renew Energy*. 2016;86:985–992.
[67] Loveridge F, Powrie W, Nicholson D. Comparison of two different models for pile thermal response test interpretation. *Acta Geotech*. 2014;9(3):367–384.
[68] Abdelaziz S, Ozudogru TY. Non-uniform thermal strains and stresses in energy piles. *Environ Geotech*. 2016;3:237–252.
[69] Corti D, Ramus M. *Soil heat transfer analysis in presence of heat exchangers embedded in foundation structures* M.S. Thesis, Italy: Politecnico di Milano; 2012: (in Italian).
[70] Sterpi D, Angelotti A, Corti D, Ramus M. Numerical analysis of heat transfer in thermo-active diaphragm walls. In: Hicks M, Brinkgreve R, Rohe A, eds. *Proc. 8th NUMGE Conf., Vol. 2*. London: Taylor & Francis Group; 2014:1043–1048.
[71] Lewis RW, Nithiarasu P, Seetharamu KN. *Fundamentals of the Finite Element Method for Heat and Fluid Flow*. John Wiley and Sons; 2004.
[72] Dassault Systèmes. Abaqus 6.14 Software Documentation. Dassault Systèmes Simulia Corp., Providence, RI, USA, 2014.
[73] Faizal M, Bouazza A, Singh RM. An experimental investigation of the influence of intermittent and continuous operating modes on the thermal behaviour of a full scale geothermal energy pile. *Geomech Energy Environ*. 2016; http://dx.doi.org/10.1016/j.gete.2016.06.002.
[74] Hillel D. Soil temperature and heat flow. In: *Introduction to Environmental Soil Physics*. Elsevier; 2003:215–233.
[75] Sterpi D, Mauri L. Thermo-mechanical finite element analyses of energy walls. In: Wuttke F, Bauer S, Sanchez M, eds. *Proc. 1st Int. Conf. Energy Geotechnics, ICEGT*. London: Taylor & Francis Group; 2016:545–550.
[76] Coletto A, Sterpi D. Structural and geotechnical effects of thermal loads in energy walls. *Procedia Eng*. 2016;158:224–229.
[77] Di Donna A, Rotta Loria A, Laloui L. Numerical study of the response of a group of energy piles under different combinations of thermo-mechanical laods. *Comput Geotech*. 2016;72:126–142.